Determination of the Dihedral Angle ψ Based on J Coupling Measurements in $^{15}N/^{13}C$-Labeled Proteins

Maurizio Pellecchia, Roberto Fattorusso, and Gerhard Wider*

Institut für Molekularbiologie und Biophysik
Eidgenössische Technische Hochschule-Hönggerberg
CH-8093 Zürich, Switzerland

Received March 12, 1998

In this communication, we propose a new three-dimensional triple-resonance NMR experiment for the determination of the ψ angles in doubly $^{13}C/^{15}N$-labeled protein samples dissolved in ^2H_2O. This experiment, referred to as 3D HCA(CO)N-*J*, resolves the small $^3J[^1H^\alpha(i),^{15}N(i+1)]$ coupling constants combining the advantages of the exclusive correlation spectroscopy (E.COSY) principle[1] with the long relaxation time of the ^{15}N nuclei in $^{15}N-^2H$ groups in a protein after a complete exchange of amide protons against deuterons in a ^2H_2O solution. These coupling constants can be correlated to the dihedral angle ψ using a Karplus relation.[2] The experimental scheme for the 3D HCA(CO)N-*J* experiment, reported in Figure 1, is similar to the HCA(CO)N experiment used for backbone resonance assignments.[3] Therefore we will only briefly describe the new features of the experiment.

The pulse sequence shown in Figure 1 starts with the α-proton magnetization on residue i, $^1H^\alpha(i)$, which is transferred by a series of INEPT (insensitive nuclei enhanced by polarization transfer) steps via the α-carbon, $^{13}C^\alpha(i)$, to the carbonyl carbon, $^{13}CO(i)$, and subsequently to the amide nitrogen of residue $(i+1)$, $^{15}N(i+1)$.[3] This ^{15}N magnetization is allowed to evolve during the period t_1 with the simultaneous application of continuous ^2H decoupling with WALTZ-16.[4] Decoupling from $^{13}C^\alpha$ and ^{13}CO spins is obtained with 180° pulses (Figure 1). Since all amide protons are exchanged against deuterons only long-range $^{15}N-^1H$ couplings influence the evolution of the ^{15}N magnetization during t_1. Using the product operator formalism,[5] omitting relaxation terms and constant multiplicative factors, the spectral density at the time point *a* in Figure 1 can be described by

$$\sigma(a) = N_y C_z' C_z \{\cos[(\omega_N + \pi^3 J_{\alpha N})t_1] + \cos[(\omega_N - \pi^3 J_{\alpha N})t_1]\}$$

where N stands for nitrogen, C' for the carbonyl carbon, and C for the α-carbon magnetization, $^3J_{\alpha N}$ denotes the $^3J[^1H^\alpha(i),^{15}N(i+1)]$ coupling constant, and ω_N is the resonance frequency of nitrogen nuclei. The magnetization described by $\sigma(a)$ is transferred back via $^{13}CO(i)$ to $^{13}C^\alpha(i)$ magnetization. This antiphase magnetization is refocused into in-phase α-carbon magnetization and simultaneously frequency labeled with the $^{13}C^\alpha$ chemical shift during the evolution time t_2, which is implemented in a constant time period of duration τ_3. During t_2 no proton decoupling is applied so that the signal is modulated by the $^1J[^{13}C^\alpha,^1H^\alpha]$ coupling. At the time point *b* the magnetization of interest can be described by

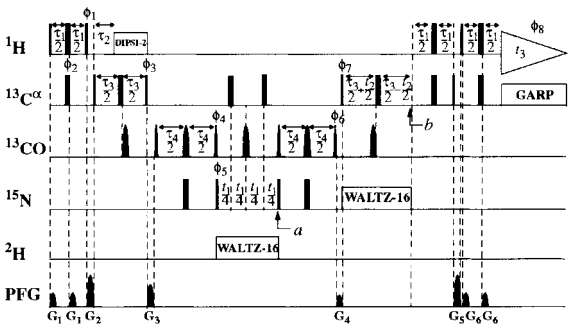

Figure 1. Experimental scheme of the 3D HCA(CO)N-*J* experiment. Thin and thick vertical bars indicate 90° and 180° pulses, respectively. The pulses on ^{13}CO have the shape of a sinc center lobe, are applied phase-modulated shifting the excitation frequency from 53 to 180 ppm, and have been optimized to avoid excitation of α-carbon magnetization. All radiofrequency (rf) pulses are applied with phase x, except when indicated otherwise above the pulse bars. The $^{13}C^\alpha$ and ^{13}CO pulses were not applied simultaneously because they are generated by the same rf channel. Pulsed field gradients (PFGs) are indicated on the line PFG and are used to dephase unwanted magnetization components including the residual solvent line.[12] The duration and amplitudes of the sine-bell-shaped PFGs are 400 μs and 30 G/cm for G_1, 1 ms and 40 G/cm for G_2, 800 μs and 20 G/cm for G_3, 800 μs and 30 G/cm for G_4, 800 μs and 40 G/cm for G_5, and 400 μs and 30 G/cm for G_6. The constant delays have the values $\tau_1 = 3.4$ ms, $\tau_2 = 3.4$ ms, $\tau_3 = 7.2$ ms, and $\tau_4 = 22$ ms. The following phase cycling scheme was applied: $\phi_1 = y, -y$; $\phi_2 = x, -x$; $\phi_3 = x, x, -x, -x$; $\phi_4 = y$; $\phi_5 = 4x, 4(-x)$; $\phi_6 = y$; $\phi_7 = 8(x), 8(-x)$; ϕ_8 (receiver) $= x, -x, -x, x, -x, x, x, -x, -x, x, x, -x, x, -x, -x, x$. Phase differences on $^{13}C^\alpha$ magnetization induced by the application of 180° ^{13}CO pulses can be compensated by a slight change of the phases ϕ_3 and ϕ_7. Quadrature detection in the indirect dimensions, t_1 and t_2, is obtained by appling the States-TPPI technique[13] with the phases ϕ_5 and ϕ_7, respectively. A DIPSI-2 sequence[14] with a strength of 1.2 kHz is applied to ^1H during the heteronuclear magnetization transfer, and a GARP sequence[15] (1.0 kHz) is employed on $^{13}C^\alpha$ during t_3. WALTZ-16 sequences[4] with strengths of 0.5 and 1.5 kHz are used to decouple ^{15}N from ^2H during t_1 and $^{13}C^\alpha$ from ^{15}N during t_2, respectively.

$$\sigma(b) = C_y\{\cos[(\omega_N + \pi^3 J_{\alpha N})t_1]\cos[(\omega_{C\alpha} + \pi^1 J_{CH})t_2] + [\cos(\omega_N - \pi^3 J_{\alpha N})t_1]\cos[(\omega_{C\alpha} - \pi^1 J_{CH})t_2]\}$$

where $^1J_{CH}$ stands for $^1J[^{13}C^\alpha,^1H^\alpha]$ and $\omega_{C\alpha}$ represents the resonance frequency of α-carbon nuclei. After time point *b* the magnetization is transferred back to $^1H^\alpha$ and detected during t_3. In the resulting spectrum the $^3J_{\alpha N}$ coupling can be measured accurately from the displacement in the ^{15}N dimension of the two multiplet components which are separated by the $^1J_{CH}$ coupling (∼140 Hz) in the ^{13}C dimension (Figure 2). Possible additional long-range couplings of ^{15}N to remote ^1H spins were omitted in the description of the experiment since they are not mutually coupled to $^{13}C^\alpha$ and thus contribute equally to both cross-peak components as a small line broadening.

Figure 2 shows slices from a 3D HCA(CO)N-*J* spectrum measured on a 1 mM sample of uniformly $^{13}C/^{15}N$-labeled 434-repressor(1−63) in ^2H_2O. Figure 2 clearly demonstrates that the $^3J_{\alpha N}$ values are accurately measurable despite of their relatively small values. The ψ angles can be determined with the Karplus relation:[2]

$$^3J[^1H^\alpha(i),^{15}N(i+1)] = -0.88\cos^2(\psi + 60°) - 0.61\cos(\psi + 60°) - 0.27$$

The $^3J_{\alpha N}$ coupling constants vary between −1.2 and −1.8 Hz in

* To whom correspondence should be addressed. Telephone: +41 1 633 34 55. Fax: +41 1 633 10 73. E-mail: gsw@mol.biol.ethz.ch.

(1) Griesinger, C.; Sørensen, O. W.; Ernst, R. R. *J. Magn. Reson.* **1987,** *75,* 474−492.
(2) Wang, A. C.; Bax, A. *J. Am. Chem. Soc.* **1995**, *117*, 1810−1813.
(3) Kay, L. E.; Ikura, M.; Tschudin, R.; Bax, A. *J. Magn. Reson.* **1990,** *89,* 496−514. Palmer, A. G.; Faibrother, W. J.; Cavanagh, J.; Wright, P. E.; Rance, M. *J. Biomol. NMR* **1992**, *2*, 103−108. Powers, R.; Gronenborn A.; Clore, G. M.; Bax, A. *J. Magn. Reson.* **1991**, *94*, 209−213.
(4) Shaka, A. J.; Keeler, J.; Frenkiel, T.; Freeman, R. *J. Magn. Reson.* **1983**, *52*, 335−338.
(5) Sørensen, O. W.; Eich, G. W.; Levitt, M. H.; Bodenhausen, G.; Ernst, R. R. *Prog. NMR Spectrosc.* **1983**, *16*, 163−192.

S0002-7863(98)00822-1 CCC: $15.00
Published on Web 06/24/1998

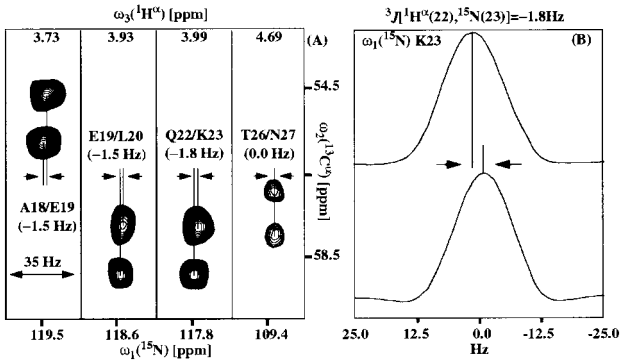

Figure 2. (A) Contour plots of four representative [$\omega_1(^{15}N)$,$\omega_2(^{13}C^\alpha)$] strips from the 3D HCA(CO)N-*J* experiment taken at the $\omega_3(^1H^\alpha)$ chemical shifts indicated at the top of the individual strips. The spectrum was obtained with a 1 mM sample of uniformly $^{13}C/^{15}N$-labeled 434-repressor(1−63) (solvent ^2H_2O, pD* = 7.0, T = 13 °C) on a Bruker DRX500 spectrometer operating at 500-MHz ^1H frequency using the pulse scheme reported in Figure 1. The four strips show sequential $^{13}C^\alpha(i)-^{15}N(i+1)$ correlations where the vertical splitting corresponds to the $^1J[^{13}C^\alpha(i),^1H^\alpha(i)]$ coupling and the horizontal displacement is the $^3J_{\alpha N}$ coupling. The assignments of the cross-peaks[16] and the measured $^3J_{\alpha N}$ coupling constants (in brackets) are indicated in the strips. The following parameters were used: the carrier for the ^1H pulses was placed on the solvent line at 4.9 ppm; the $^{13}C^\alpha$, ^{15}N, and ^2H carriers were set to 53, 116, and 8.0 ppm, respectively. 90° pulse lengths of 8 μs for ^1H, 48 μs for ^{15}N, 65 μs for $^{13}C^\alpha$, and 106 μs for ^{13}CO were used. 180° pulses were applied with the same rf power as for the 90° pulses. With these parameters, no significant phase correction for the phases ϕ_3 and ϕ_7 was needed (see caption for Figure 1). The 3D spectrum was recorded in 2 days with 128 × 16 × 512 complex points in the t_1, t_2, and t_3 dimensions, respectively, yielding $t_{1,max}(^{15}N)$ = 102.4 ms, $t_{2,max}(^{13}C)$ = 7.2 ms, and $t_{3,max}(^1H)$ = 85.2 ms. Linear prediction and mirror image linear prediction[17] were performed in the ^{15}N and ^{13}C dimensions, respectively, doubling the time domain size in these dimensions. After zero-filling, the following digital resolutions were achieved: 19.6 Hz (^{13}C), 0.6 Hz (^{15}N), 11.7 Hz (^1H). The spectrum was processed with the program PROSA[18] and analyzed with the program XEASY.[19] (B) Cross sections parallel to $\omega_1(^{15}N)$ through the peaks in the strip of Q22/K23 in panel A.

α-helical regions, whereas very small couplings in the range from +0.1 to −0.5 Hz are expected in β-sheet regions.[2]

The use of the E.COSY principle requires that the $^1H^\alpha$ nuclear spin does not change its state between the evolution time periods t_1 and t_2 (Figure 1). In practice, nuclear spin relaxation influences the $^1H^\alpha$ spin states with the consequence that the size of the apparent value for $^3J_{\alpha N}$ is slightly reduced.[6,8] However, with all amide protons exchanged against deuterons, the $^1H^\alpha$ nuclei relax slower due to the missing $^1H^\alpha-^1H^N$ dipole−dipole interaction[7] so that the use of $^1H^\alpha$ as passive spin does not represent a disadvantage and the reduction of the values for $^3J_{\alpha N}$ is negligible.

In the alternative experiments HN(CO)CA-*J*[8] and HCACO-[N]-E.COSY,[2] the $^3J_{\alpha N}$ coupling constants are measured by small cross-peak displacements in the ^{15}N and $^1H^\alpha$ dimensions, respectively. The new 3D HCA(CO)N-*J* (Figure 1) presents crucial advantages over these methods. With all amide protons exchanged against deuterons, there is no disturbance from the large $^1J[^{15}N,^1H^N]$ coupling constants during t_1, and therefore, no selective $^1H^N$ decoupling, as for example in the HN(CO)CA-*J* experiment,[8] is required. Moreover, a very high ^{15}N resolution can be achieved due to the prolonged transverse relaxation time of the ^{15}N nuclei bound to ^2H instead of ^1H, when the ^{15}N nuclei are decoupled from ^2H (Figure 1). In this case, ^{15}N nuclei represent a preferable choice to resolve the rather small $^3J_{\alpha N}$ coupling constants, exhibiting a resolution usually not obtainable when detecting on the α-proton as, for example, in the HCACO-[N]-E.COSY.[2] The latter is in principle a 2D experiment which requires a relatively high resolution in the indirect dimension to resolve the small $^1J[^{13}CO,^{15}N]$ coupling (∼15 Hz). However, in the 3D HCA(CO)N-*J* experiment, only low resolution in the $^{13}C^\alpha$ dimension is necessary to resolve the large $^1J_{CH}$ coupling (∼140 Hz). The overall size of the data matrices and sensitivity in the two experiments are comparable. However, the large $^1J_{CH}$ coupling can still be resolved in larger molecules, whereas this is no longer possible for the small $^1J[^{13}CO,^{15}N]$ couplings.

In conclusion, the novel experiment 3D HCA(CO)N-*J* provides easily accessible information on ψ angles also because there is no overlap of the values for $^3J_{\alpha N}$ between α-helical and β-sheet regions. This experiment may therefore also be preferable to the recently developed method based on cross-correlation between the $^1H-^{13}C^\alpha$ dipolar and the carbonyl chemical shift anisotropy relaxation,[9] that is up to 4-fold degenerate for ψ values of 180°, and to the direct measurement of intervector angles between CH-(i) and NH($i+1$) bonds,[10] where the necessary knowledge of the correlation time may constitute an additional source of uncertainty. The information obtained from the new experiment could also well complement those obtained from the recently proposed empirical correlation between ψ angles and deuterium isotope shifts where smaller shifts are observed for residues in α-helical regions and larger shifts in β-sheets.[11]

Acknowledgment. Financial support was obtained from the Schweizerischer Nationalfonds (Project 31.32033.91), from an EMBO fellowship for M.P., and from "Seconda Universita' degli Studi di Napoli" for R.F. We thank Prof. Dr. K. Wüthrich and Dr. P. Güntert for helpful discussions and Dr. G. Siegal for providing the NMR sample used in this work.

Supporting Information Available: Figure comparing the ψ angles obtained from the measurements of the $^3J_{\alpha N}$ coupling constants and the angles in the three-dimensional NMR structure of the N-terminal domain of 434-repressor (residues 1−63) and a list of the measured $^3J_{\alpha N}$ values (2 pages, print/PDF). See any current masthead page for ordering information and Web access instructions.

JA980822K

(6) Wang, A. C.; Bax, A. *J. Am. Chem. Soc.* **1996**, *118*, 2483−2494.
(7) Nietlispach, D.; Clowes, R. T.; Broadhurst, R. W.; Ito, Y.; Keeler, J.; Kelly, M.; Ashurst, J.; Oschkinat, H.; Domaille, P. J.; Laue, E. *J. Am. Chem. Soc.* **1996**, *118*, 407−415.
(8) Seip, S.; Balbach, J.; Kessler, H. *J. Magn. Reson. B* **1994**, *104*, 172−179.
(9) Yang, D.; Konrat, R.; Kay, L. E. *J. Am. Chem. Soc.* **1997**, *119*, 11938−11940.
(10) Rief, B.; Henning, M.; Griesinger, C. *Science* **1997**, *276*, 1230−1233.
(11) Ottiger, M.; Bax, A. *J. Am. Chem. Soc.* **1997**, *119*, 8070−8075.
(12) Bax, A.; Pochapsky, S. S. *J. Magn. Reson.* **1992**, *99*, 638−643. Wider, G.; Wüthrich, K. *J. Magn. Reson. B* **1993**, *102*, 239−241.
(13) Marion, D.; Ikura, K.; Tschudin, R.; Bax, A. *J. Magn. Reson.* **1989**, *85*, 393−399.
(14) Shaka, A. J.; Lee, C. J.; Pines, A. J. *J. Magn. Reson.* **1988**, *77*, 274−293.
(15) Shaka, A. J.; Barker, P. B.; Freeman, R. *J. Magn. Reson.* **1985**, *64*, 547−552.
(16) Pervushin, K.; Billeter, M.; Siegal, G.; Wüthrich, K. *J. Mol. Biol.* **1996**, *264*, 1002−1012.
(17) Zhu, G.; Bax, A. *J. Magn. Reson.* **1990**, *90*, 405−410.
(18) Güntert, P.; Dötsch, V.; Wider, G.; Wüthrich, K. *J. Biomol. NMR* **1992**, *2*, 619−629.
(19) Bartels, C.; Xia, T. H.; Billeter, M.; Güntert, P.; Wüthrich, K. *J. Biomol. NMR* **1995**, *6*, 1−10.